Flow (2024), **4** E12
doi:10.1017/flo.2024.10

FLOW CAMBRIDGE UNIVERSITY PRESS

RESEARCH ARTICLE

The configurational entropy of pillar-arrayed microstructured surfaces with spreading droplets

Enhui Chen[1,2,3], Xianfu Huang[1,2] and Ya-Pu Zhao[1,2,*]

[1]State Key Laboratory of Nonlinear Mechanics, Institute of Mechanics, Chinese Academy of Sciences, Beijing 100190, PR China
[2]School of Engineering Science, University of Chinese Academy of Sciences, Beijing 100049, PR China
[3]School of Physical Science and Engineering, Beijing Jiaotong University, Beijing 100044, PR China
*Corresponding author. E-mail: yzhao@imech.ac.cn

Received: 22 February 2024; **Revised:** 28 April 2024; **Accepted:** 12 May 2024

Keywords: Droplet; Spreading; Configurational entropy; Microstructured surface

Abstract

Microstructured surfaces with pillar arrays are widely used to control the wetting morphology and spreading dynamics of droplets. In both simulations and experiments, it is shown that fabricating the surface with various microstructures is a very effective method for achieving the desired symmetry of the moving contact line. However, the method for characterizing miscellaneous pillar-arrayed microstructured surfaces is still insufficient. This paper presents the configurational entropy to characterize the microstructured surfaces with pillar arrays. By calculating the configurational entropy of pillar-arrayed microstructured surfaces, the relationship between the configurational entropy and the wetting morphology of droplets is obtained. For pillar-arrayed microstructured surfaces with the configurational entropy $S > 0$, the droplet wetting morphology may be much more complex than those with $S = 0$. The relationship is found to be consistent with the previous results. Furthermore, the wetting dynamics has been analysed. This study may be useful to understand the mechanism of droplet wetting on pillar-arrayed microstructured surfaces and provide insights for the design and manufacture of microstructured surfaces.

Impact Statement

A method for characterizing pillar-arrayed microstructured surfaces has been given. The concept of configurational entropy for pillar-arrayed microstructured surfaces has been introduced, and a detailed calculation has been provided. Subsequently, the values of configurational entropy for both periodically and quasiperiodically patterned pillar-arrayed surfaces have been calculated. The wetting morphology of liquid droplets on both periodically patterned pillar-arrayed surfaces and quasiperiodically patterned pillar-arrayed surfaces has been summarized. The influence of configurational entropy of surfaces on the wetting morphology and dynamics of liquid droplets in experiments has been discussed. The results may advance the control capability of complex wetting morphology, and are helpful in applications of microfluidics, self-cleaning materials, inkjet and 3D printing, etc.

1. Introduction

Liquid droplets spreading on solid surfaces are ubiquitous in both nature and practical applications, such as plant leaves, electrocapillary peeling (Li, Huang & Zhao 2023*a*), dielectrophoresis (Bercovici *et al.*

2021), 3D printing (Yuk *et al.* 2020), energy/water harvesting (Chen *et al.* 2018*a*; Yu *et al.* 2020; Li *et al.* 2023*b*), microfluidics (Wang *et al.* 2014*a*; Yang *et al.* 2021; Li, Huang & Zhao 2022), ink-jet printing (Wang *et al.* 2014*b*; Brockmann *et al.* 2024), self-cleaning (Singh *et al.* 2010), etc. In these applications, the ability to control the morphology of the wetted area, that is, the morphology of the moving contact line, is of significant importance because the morphology is closely related to the fabrication process (Yu *et al.* 2021). Over the past few decades, researchers have devoted significant attention to this matter, yielding abundant results though experimentation, simulation and theoretical investigation. It has been found that the morphology of the wetted area of droplets is closely related to both the topology of rough surfaces and the liquid properties (Cazabat & Stuart 1986, 1987; Apel-Paz & Marmur 1999; Alberti & DeSimone 2005; Quéré 2008; Chamakos *et al.* 2016; Zhao 2016; Wang *et al.* 2021). Surface chemical moderating techniques (Jain & Pitchumani 2017) and surface roughness preparation methods (Raj *et al.* 2012), particularly in the fabrication of surfaces with micropillars, are extensively employed (Courbin *et al.* 2007; Jokinen, Leinikka & Franssila 2009; Chu, Xiao & Wang 2010; Lv *et al.* 2010; Xiao, Enright & Wang 2010; Xiao & Wang 2011) to achieve the desired morphology of the wetted area of liquid droplets.

The method of fabricating roughness on solid surfaces is more stable than that of chemical moderating solid surfaces (Duprat *et al.* 2012). Additionally, topology, roughness and geometry parameters can be designed in the method of fabricating microstructures on solid surfaces. As a result, the method of fabricating microstructures on solid surfaces gradually received more attention than that of chemical moderating solid surfaces (Courbin *et al.* 2007; Lv *et al.* 2010; Xiao *et al.* 2010; Kim *et al.* 2011).

The characterization method of rough surfaces has been studied since the last century. In fact, solid surfaces in nature are usually rough. A common example is a rock's surface, on which the phenomenon of liquid droplet spreading has been pioneered by de Gennes (Dufour *et al.* 2012). Such a rough surface is called a fractal surface (de Gennes 1985), and the roughness of a fractal surface is $(L/l)^{\xi-2}$, where L and l denote the largest and smallest sizes of the fractal surface, respectively. Besides the definition of surface roughness, fractal dimension (Packham 2003) has also been proposed to characterize the disorder of rough surfaces. In the experiments, a rough surface can be prepared on a smooth glass surface by using different grades of abrasive powder and sand blasting (Mandelbrot 1918; Cazabat & Stuart 1987). The characterization is usually the amplitude and the quadratic variation of the surface. However, the roughness of such a rough surface is random, and there is a lack of accurate characterization of the rough surface.

To model the pillar-arrayed microstructured surfaces, micropillars have been extensively used in recent decades. It is proved that the distribution parameters of micropillars on solid surfaces such as symmetry, density, roughness, height and the morphology of pillars, are all related to the morphology of the wetting area of liquid droplets on these surfaces (Cazabat & Stuart 1986; Courbin *et al.* 2007). Liquid droplets of partial wetting on a smooth lyophilic surface may become complete wetting on a pillar-arrayed microstructured surface (Quéré 2008; Zhao 2012; Chen *et al.* 2016). For example, by fabricating a square array of micropillars on a solid surface, the droplets are more likely to spread into a square wetted area rather than circular ones (Zhao 2014). By using soft-lithography techniques or/and reactive ion etching processes, the size of the micropillars can be controlled from several micrometres to tens of micrometres in experiments. Therefore, as the size of the micropillars decreases, the roughness of the micropillars increases dramatically. On the microstructured surface with small pillars, the morphology of the wetted area of a spreading droplet is strongly affected by the micropillars. The droplets can even spread into a bilayer structure (Extrand *et al.* 2007). This means that the bottom of the droplet spreads within the pillars, forming a so-called fringe film, and the upper part of the droplet is above the pillars, which is called a bulk droplet. Liquid droplets with square projected fringe shape and circular projected bulk shape, octagonal projected fringe shape with circular projected bulk shapes, square projected fringe shape, octagonal projected fringe shape, circular fringe with circular projected bulk shapes, etc, have appeared on square arrayed micropillar surfaces (Chen *et al.* 2016). By changing the symmetry of the surface array to a rectangle, liquid droplets with a rectangular and stretched octagonal wetted area can be obtained (Courbin *et al.* 2007). In the same way, by changing the symmetry of the surface

https://doi.org/10.1017/flo.2024.10 Published online by Cambridge University Press

array to a hexagon, it is possible to obtain droplets with a hexagonal wetted area (Raj *et al.* 2014). And droplets with a dodecagonal wetted area can be achieved on a pillar-arrayed surface with a hexagonal array (Courbin *et al.* 2009). Among the above-mentioned studies, the symmetry of the various wetted areas of the droplets coincide with the symmetry of the pillar arrays on the microstructured surface. The wetted shapes of droplets on the square arrayed surface with four-fold symmetry, both square and octagon, are four-fold symmetric; the wetted shape of droplets on the rectangular arrayed surface with two-fold symmetry, including rectangular and stretched square, are two-fold symmetric; and similarly, the wetted shape of droplets on a hexagonal arrayed surface with six-fold symmetry, i.e. dodecagon and hexagon, are both six-fold symmetric.

Besides research on periodically patterned surfaces with two-, four- and six-fold symmetry (Raj *et al.* 2014), it is noteworthy that quasiperiodically patterned surfaces have also been investigated (Chen, Yuan & Zhao 2018*b*). On such surfaces, the symmetry of the wetted area of droplets can decrease and restore spontaneously. For example, it is reported that on the surface with a five-fold quasiperiodically pattern, the symmetry of the wetted area of the droplets can be circular, five-fold, or ten-fold. And on six-fold quasiperiodically patterned surfaces, the symmetry of the wetted area of the droplets can be circular, six-fold or twelve-fold. This indicates a distinct difference between periodically patterned and quasiperiodically patterned surfaces. Nevertheless, there is currently a lack of characterization of pillar-arrayed micropatterned surfaces due to the inability of roughness, symmetry and the geometry parameters to differentiate between the two kinds of surfaces.

In this work, a calculating method of configurational entropy of the pillar-arrayed surfaces is given to characterize the degree of disorder of micropillars. The configurational entropy of commonly used pillar-arrayed micropatterned surfaces has been calculated and compared with the morphology transition of the wetted area of the droplets. It is found that the configurational entropy proposed in this study can describe the pillar-arrayed microstructured surface to some extent.

2. Problem

As mentioned in § 1, the characterization method for rough surfaces, particularly for pillar-arrayed microstructured surfaces includes surface roughness, the pillar density, aspect ratios and symmetry. The definition of surface roughness, *ro,* is described as the ratio of the actual area of solid surface, S_{ac}, to the projected area of solid surface, S_p (Chen *et al.* 2018*b*),

$$ro = \frac{S_{ac}}{S_p}. \tag{2.1}$$

According to this definition, the surface roughness is a constant on uniformly patterned pillar-arrayed surfaces, but a function of location on surfaces with non-uniform structures.

The definition of pillar density (Quéré 2008), which is referred to as the density of defects or the surface area fraction of a solid surface (McHale *et al.* 2009), is defined as the ratio of the projected area of the rough solid surface to the projected area of the total solid surface (Yuan & Zhao 2013),

$$\phi_s = \frac{S_r}{S_p}. \tag{2.2}$$

Similar to surface roughness, *ro*, the pillar density of a solid surface or the surface area fraction of a solid surface is also a constant on uniformly patterned pillar-arrayed surfaces, but a function of location on surfaces with non-uniform structures.

The definition of aspect ratio is described as the ratio of height of a pillar, *h,* to the inner distance of pillars, *l* (McHale *et al.* 2009),

$$A_i = \frac{h}{l}, \tag{2.3}$$

https://doi.org/10.1017/flo.2024.10 Published online by Cambridge University Press

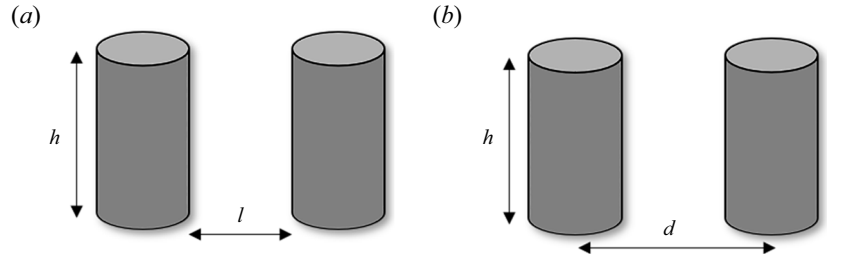

Figure 1. *Illustration of aspect ratio of the pillars on surfaces. (a) The aspect ratio of A_i, which is the ratio of the height of a pillar h to the inner distance of pillars l (Raj et al. 2014). (b) The aspect ratio of A_p, which is the ratio of the height of a pillar h to the period of pillars d (Courbin et al. 2007).*

as illustrated in figure 1(*a*). In some cases, the definition of aspect ratio is described as the ratio of height of a pillar, *h,* to the period of pillars, *d* (Courbin *et al.* 2007),

$$A_p = \frac{h}{d}, \tag{2.4}$$

as illustrated in figure 1(*b*).

The symmetry of a pillar-arrayed microstructured surface could be identified by the topography of the array. While these methods of characterization have been proven effective in describing wetting, spreading morphology and dynamics in previous studies (Yuan & Zhao 2013; Raj *et al.* 2014; Yuan, Huang & Zhao 2014), the shortage arises when the quasiperiodically patterned surfaces fabricated with micropillars are used to control the morphology of moving contact lines of liquid droplets. The roughness and pillar density of quasiperiodically patterned surfaces fabricated with micropillars exhibit variation in the short range with location, but remain constant in the long range (Stampfli 1986; Kumar & Raj 2017) due to the characteristic of being disordered in the short range but ordered in the long range. Additionally, aspect ratios fail to adequately characterize quasiperiodically patterned surfaces fabricated with micropillars due to the disorder feature in the short range. Moreover, symmetry alone could not effectively characterize quasiperiodically patterned surfaces fabricated with micropillars, as certain types of quasiperiodically patterned surfaces exhibit the same symmetry as periodically patterned surfaces fabricated with micropillars arranged in an array. Thus, there is a need for a further characterization method of a pillar-arrayed surface.

3. Description

Firstly, the nearest-neighbour distance of pillars on a pillar-arrayed microstructured surface is defined. This approach simplifies each pillar to a dot, ignoring their size and shape, thus defining the nearest neighbour distance as the distance between one dot and its closest neighbour. Pillars on a microstructured surface arranged in a pillar array may exhibit variations in both the nearest neighbour distances and the number of nearest neighbour pillars. Considering pillars with identical nearest neighbour distances and numbers of nearest neighbour as one kind may result in multiple kinds of pillars on one surface. Then let i denote one kind of pillar, which has the same nearest neighbour distance and number of nearest neighbour pillars, c_i denote the ratio of the number of i kinds of pillar to the number of all pillars on the surface and N denote the number of kinds of pillars. Thus, a formula can be derived as

$$\sum_{i=1}^{N} c_i = 1, \tag{3.1}$$

which means the sum of ratios of all kinds of pillars is equal to 1.

https://doi.org/10.1017/flo.2024.10 Published online by Cambridge University Press

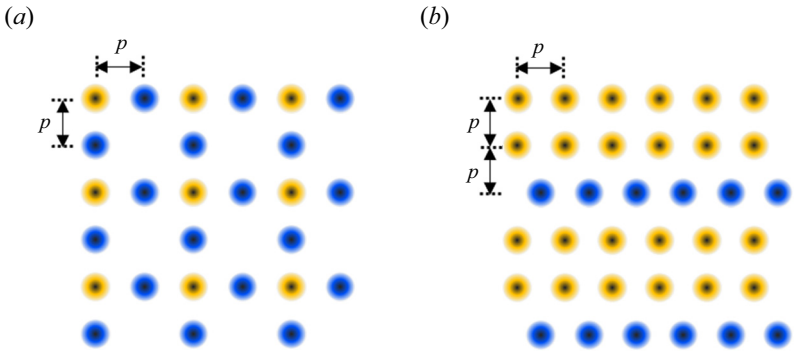

Figure 2. *Illustration of configurational entropy on pillar-arrayed microstructured surfaces. Each dot denotes a pillar, each colour represents one kind of pillar on a surface and p denotes the distance between pillars. The pillars on surfaces are arranged periodically.*

Using i, c_i and N, the configurational entropy, S, of a pillar-arrayed microstructured surface is given by

$$S = -\sum_{i=1}^{N} c_i \ln c_i. \tag{3.2}$$

Here, the configurational entropy was given to characterize the geometry of a micro-pillar-arrayed surface.

4. Examples

We take figure 2 as an example to illustrate the kinds of pillars and the configurational entropy of pillar-arrayed microstructured surfaces. Note that in figure 2 the pillars, which are represented by two-dimensional dots, are arranged periodically.

In figure 2(*a*), each yellow dot has four nearest neighbour dots with the nearest neighbour distance of p. Meanwhile, each blue dot has two nearest neighbour dots with the nearest neighbour distance of p. Consequently, the yellow dots are classified as one kind and the blue dots as another. Considering the periodically patterned surface, the ratio of yellow dots, denoted as c_1, is calculated to be 0.33, and the ratio of blue dots, denoted as c_2, is calculated to be 0.67. As a result, the configurational entropy of the surface in figure 2(*a*) is calculated to be 0.64.

In figure 2(*b*), each yellow dot has three nearest neighbour dots with the nearest neighbour distance of p. Meanwhile, each blue dot has two nearest neighbour dots with the nearest neighbour distance of p. Thus, the yellow dots are one kind and the blue ones another kind. Considering the periodical surface, the ratio of yellow dots c_1 is calculated to be 0.67, and the ratio of blue dots c_2 is calculated to be 0.33. As a result, the configurational entropy of the surface in figure 2(*b*) is calculated to be 0.64.

5. Results and discussion

To elucidate the relationship between the wetting morphology of liquid droplets and the pillar-arrayed microstructured surfaces, it is necessary to calculate the configurational entropy of pillar-arrayed microstructured surfaces. We first focus on the periodically patterned pillar-arrayed surfaces. Such surfaces, which are employed to manipulate the morphology of liquid droplets with complete wetting, are illustrated in figure 3(*a*). In figure 3(*a*), periodically patterned surfaces fabricated with square arrayed square pillars, square arrayed circular pillars, rectangular arrayed circular pillars, hexagonal arrayed circular pillars and stretched hexagonal arrayed circular pillars are illustrated. Using the method of

https://doi.org/10.1017/flo.2024.10 Published online by Cambridge University Press

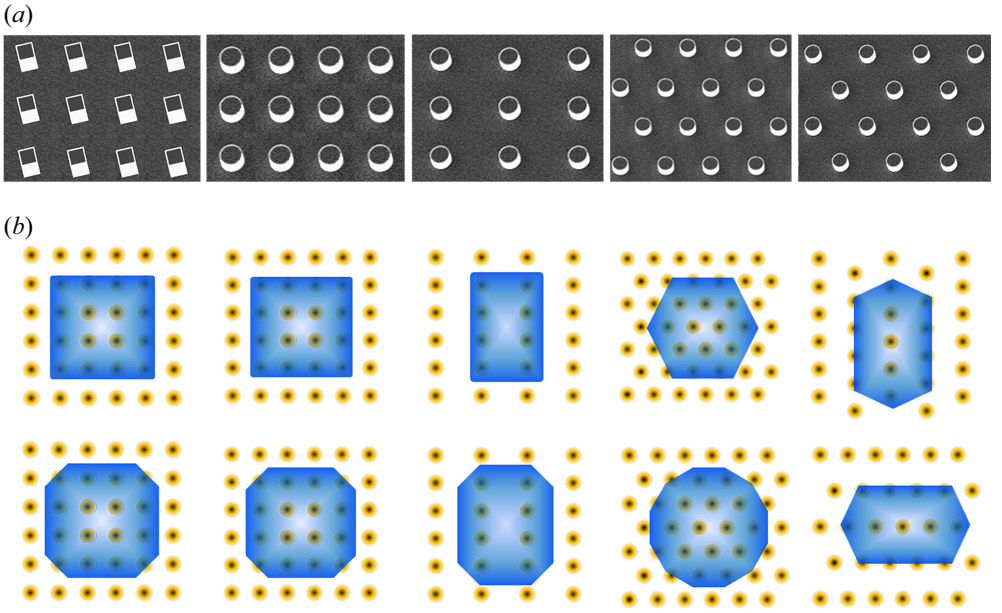

Figure 3. *(a) Illustrations of periodically patterned pillar-arrayed surfaces. (b) The wetting morphology of liquid droplets (blue polygons) on corresponding surfaces (the yellow dots denote micropillars) according to the experimental results in, e.g. Courbin et al. (2007), Raj et al. (2014) and Chen et al. (2016).*

calculating configurational entropy, it is found that the configurational entropy of each periodically patterned surface in figure 3(*a*) is zero, since the pillars on each periodically patterned surface have the same nearest neighbour distance and the number of nearest neighbour pillars.

The wetting morphology on periodically patterned pillar-arrayed surfaces, which may be inferred from the experimental findings such as those in Courbin *et al.* (2007), Raj *et al.* (2014) and Chen *et al.* (2016), has been depicted in figure 3(*b*). Note that complete wetting liquid droplets on the surfaces are considered here. In addition to the initial circular projected wetted area of a liquid droplet, the possible symmetries of the wetted area can be four-fold, four-fold, two-fold, six-fold and two-fold from left to right, which are consistent with the symmetry of periodically patterned pillar-arrayed surface.

After discussion of periodically patterned pillar-arrayed surfaces, the quasiperiodically patterned pillar-arrayed surfaces are then discussed. Such quasiperiodically patterned pillar-arrayed surfaces, employed to manipulate the morphology of wetting liquid droplets are illustrated in figure 4(*a–c*), with pillars represented as colourful dots. In figure 4(*a–c*), quasiperiodically patterned surfaces fabricated with circular pillars of five-fold, six-fold and eight-fold symmetry, respectively, are depicted (Chen *et al.* 2018*b*). Each colour denotes one kind of pillar.

Seen from figure 4(*a*), each cyan dot has two nearest neighbour dots with the nearest neighbour distance of 0.62*a* (*a* denotes the distance from the pillar at symmetric centre to the nearest neighbour pillar), each magenta dot has three nearest neighbour dots with the nearest neighbour distance of 0.62*a*, each yellow dot has five nearest neighbour dots with the nearest neighbour distance of 0.62*a*, and each black dot has 10 nearest neighbour dots with the nearest neighbour distance of *a*. Considering the structural characteristics of the five-fold symmetric quasiperiodic surface described by Chen *et al.* (2016) (also refer to figure A(a) in the supplementary material available at https://doi.org/10.1017/flo.2024.10), the ratio of cyan dots c_1 is calculated to be 0.18, the ratio of magenta dots c_2 is calculated to be 0.71, the ratio of yellow dots c_3 is calculated to be 0.02 and the ratio of black dots c_4 is calculated to be 0.09. As a result, the configurational entropy of the five-fold symmetric quasiperiodical surface is calculated to be 0.85.

https://doi.org/10.1017/flo.2024.10 Published online by Cambridge University Press

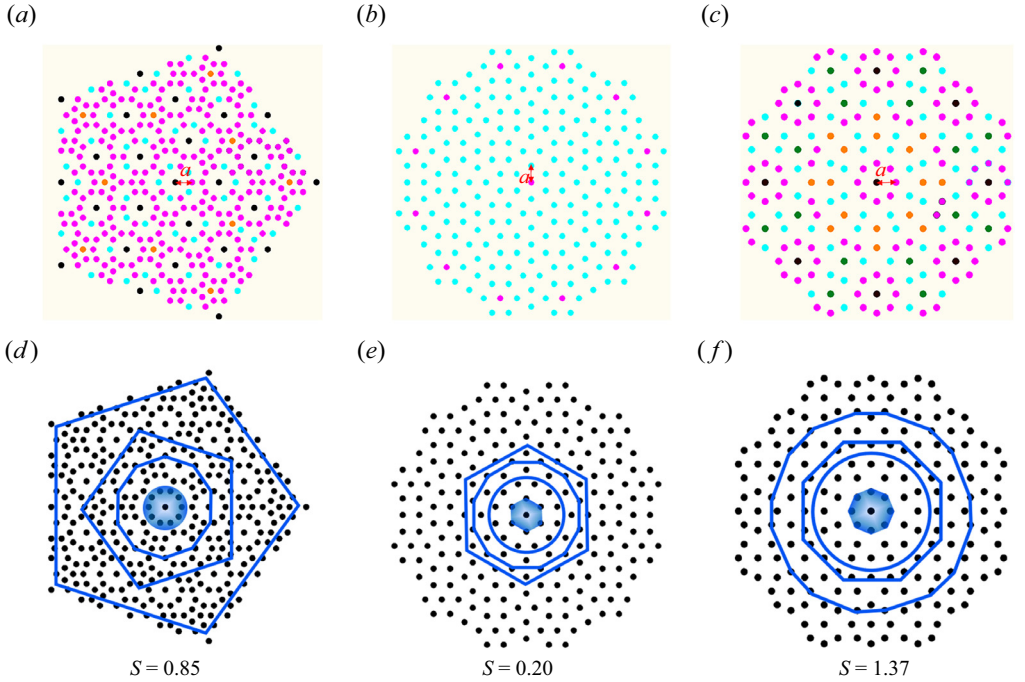

Figure 4. *(a–c) Illustrations of quasiperiodically patterned pillar-arrayed surfaces: (a) five-fold; (b) six-fold; (c) eight-fold symmetry. The length of a in each illustration denotes the distance from the pillar at the symmetric centre to the nearest neighbour pillar. Colourful circular dots represent micropillars, and each colour in each illustration represent a special kind of pillar. (d–f) The wetting morphology of liquid droplets (blue polygons) on corresponding surfaces (the black dots denote micropillars) according to the experimental results in Chen et al. (2018b).*

Seen from figure 4(*b*), each cyan dot has five nearest neighbour dots with the nearest neighbour distance equal to a, and each magenta dot has six nearest neighbour dots with the nearest neighbour distance of a. Considering the structural characteristics of the six-fold symmetric quasiperiodical surface (Penrose 1979) (also see figure A(b) in the supplementary material), the ratio of cyan dots c_1 is calculated to be 0.95, and the ratio of magenta dots c_2 is calculated to be 0.05. As a result, the configurational entropy of the six-fold symmetric quasiperiodical surface in figure 4(*b*) is calculated to be 0.20.

Seen from figure 4(*c*), each the cyan dot has one nearest neighbour dot with the nearest neighbour distance of $0.77a$, each magenta dot has two nearest neighbour dots with the nearest neighbour distance of $0.77a$, each yellow dot has five nearest neighbour dots with the nearest neighbour distance of a, each green dot has six nearest neighbour dots with the nearest neighbour distance of a and each black dot has eight nearest neighbour dots with the nearest neighbour distance of a. Considering the structural feature of an eight-fold symmetric quasiperiodical surface (Stampfli 1986) (also see figure A(c) in the supplementary material), the ratio of cyan dots c_1 is calculated to be 0.24, the ratio of magenta dots c_2 is calculated to be 0.45, the ratio of yellow dots c_3 is calculated to be 0.15, the ratio of green dots c_4 is calculated to be 0.12 and the ratio of black dots c_5 is calculated to be 0.04. As a result, the configurational entropy of the surface in figure 4(*c*) is calculated to be 1.37. The calculated values of configurational entropy are summarized in table 1.

The wetting morphology on quasiperiodically patterned pillar-arrayed surfaces (Beenker 1982), as observed in the experimental findings of Chen *et al.* (2018*b*), has been depicted in figure 4(*d–f*). On quasiperiodically patterned pillar-arrayed surfaces arranged with five-fold symmetry, as depicted in figure 4(*d*), the projected wetted area of a liquid droplet can exhibit circular, decagonal and pentagonal

https://doi.org/10.1017/flo.2024.10 Published online by Cambridge University Press

Table 1. *The values of configurational entropy S of different kinds of pillar-arrayed surfaces.*

	Periodically patterned surfaces			Quasiperiodically patterned surfaces		
Pillar-arrayed surfaces	figure 3	figure 2(*a*)	figure 2(*b*)	Five-fold	Six-fold	Eight-fold
N	1	2	2	4	2	5
S	0	0.64	0.64	0.85	0.20	1.37

shapes, indicating that the symmetry of the projected wetted area can be axisymmetric, ten-fold and five-fold, respectively. On quasiperiodically patterned pillar-arrayed surfaces of six-fold symmetry, seen from figure 4(*e*), the projected wetted area of liquid droplet can be a hexagon, circle and dodecagon, which means that the symmetry of the projected wetted area can be six-fold, axisymmetric and twelve-fold. On quasiperiodically patterned pillar-arrayed surfaces of eight-fold symmetry, seen from figure 4(*f*), the projected wetted area of liquid droplet can be an octagon, circle and hexadecagon, which means that the symmetry of the projected wetted area can be eight-fold, and axisymmetric. Clearly, the wetting morphology on quasiperiodically patterned pillar-arrayed surfaces is more complex and diverse compared with that on periodically patterned pillar-arrayed surfaces.

The wetting morphology on both periodically and quasiperiodically patterned pillar-arrayed surfaces was clarified in figure 5(*a*). To quantify the relationship between pillar-arrayed surfaces and the complexity of the wetting morphology of liquid droplets, the configurational entropy, *S,* of pillar-arrayed surfaces and the number of the symmetries, N_s, of the projected wetted area of liquid droplets are shown in figure 5(*b*). From figure 5(*b*), one can find that once the configurational entropy is higher than 0, the number of symmetries of the projected wetted area of liquid droplets will be more than 1, indicating complex transition in the wetting process. Since the arrangement of pillars in the short range significantly influences the number of symmetries, as indicated in figure 4(*d–f*), the relationship between configurational entropy and the number of symmetries is nonlinear. However, the conclusion is clear that $N_s > 1$ if $S > 0$. This may imply that the configurational entropy proposed in this work can be used to characterize the pillar-arrayed microstructured surfaces roughly. Although there is a lack of high precision, configurational entropy may be an effective method for characterizing the pillar-arrayed microstructured surfaces in some ways.

In order to further investigate the physics of surfaces with varying configurational entropy, the wetting dynamics is analysed. The wetting dynamics of a uniform and incompressible liquid can be described by the Navier–Stokes equations,

$$\boldsymbol{\nabla} \cdot \boldsymbol{v} = 0, \tag{5.1}$$

$$\frac{\partial \boldsymbol{v}}{\partial t} + (\boldsymbol{v} \cdot \boldsymbol{\nabla})\boldsymbol{v} = -\frac{1}{\rho}\boldsymbol{\nabla} p + \nu \nabla^2 \boldsymbol{v} + \boldsymbol{F}, \tag{5.2}$$

where $\boldsymbol{\nabla}$, $\boldsymbol{v}$, t, p, ρ, ν and $\boldsymbol{F}$ denote the Hamiltonian operator, velocity, time, pressure, density, kinematic viscosity and volume force, respectively. Surface tension on the liquid–gas interface becomes significant when the droplet is sufficiently small. Consequently, the force on the liquid–gas surface under the isothermal assumption can be expressed as

$$\boldsymbol{f} = \gamma(\boldsymbol{\nabla} \cdot \boldsymbol{n})\boldsymbol{n}, \tag{5.3}$$

where γ and $\boldsymbol{n}$ denote surface tension and unit normal vector on the liquid–gas interface.

Considering the roughness of the surface, the rate of change in the driving energy can be determined as

$$E_D \sim [(\gamma_{sg} - \gamma_{sl})ro - \gamma \cos\theta]\dot{R}, \tag{5.4}$$

https://doi.org/10.1017/flo.2024.10 Published online by Cambridge University Press

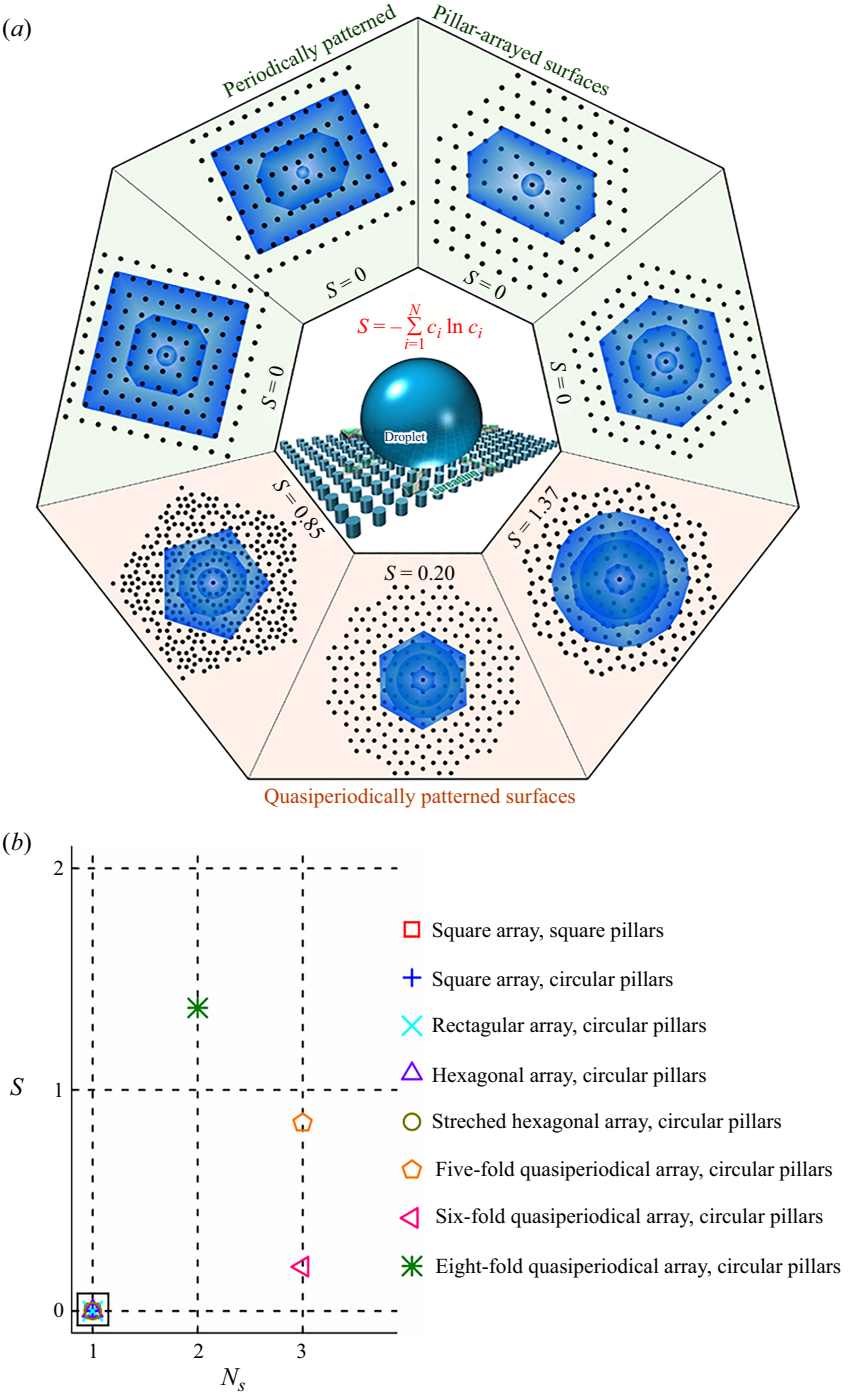

Figure 5. *(a) The wetting morphology on both periodically and quasiperiodically patterned pillar-arrayed surfaces. (b) The phase diagram of the relationship between the configurational entropy S of pillar-arrayed surfaces and the number of the symmetries N_s of projected wetted area of liquid droplets. The black square indicates $S = 0$. For the cases of $S = 0$, $N_s = 1$ and for the cases of $S > 0$, $N_s > 1$.*

https://doi.org/10.1017/flo.2024.10 Published online by Cambridge University Press

where γ_{sg}, γ_{sl}, θ and R are the solid–gas, solid–liquid interfacial tension, instant contact angle and average radius of the polygonal moving contact line. Using lubrication approximation, the scale becomes

$$E_D \sim \gamma \dot{R} \theta^2. \tag{5.5}$$

Depending on the properties of the liquids and the roughness and configurational entropy of pillar-arrayed microstructured surfaces, the rate of change in the dissipation energy of the moving contact line may be determined as (Yuan *et al.* 2014; Chen *et al.* 2016, 2018*b*)

$$E_r \sim \dot{R}^2 \zeta \text{ when molecular friction takes priority,} \tag{5.6}$$

$$E_r \sim \rho \nu \dot{R}^2 / \theta \text{ when viscous takes priority,} \tag{5.7}$$

$$E_r \sim \rho \nu h \dot{R}^2 / R \text{ on quasiperiodical surface with } S > 0. \tag{5.8}$$

Here, ζ denotes the coefficient of molecular friction. By comparing (5.6)–(5.8), it is evident that the dissipation energy scale of quasiperiodic surfaces with $S > 0$ differs significantly from that of periodic surfaces. This discrepancy can be attributed to the feature that the quasiperiodical surface with $S > 0$ is disorder in the short range but order in the long range. These theoretical predictions are validated through experiments by measuring the rate of increase in wetted area. Note that (5.8) is shown to be valid for quasiperiodic surfaces with moderate roughness and liquid viscosity. Further research may be carried to elucidate the geometric effects of the pillars on dissipation energy.

6. Conclusions

Firstly, a method for characterizing pillar-arrayed microstructured surfaces has been introduced. Configurational entropy of pillar-arrayed microstructured surfaces has been proposed and the detailed calculation has been put forward. Subsequently, the values of configurational entropy for both periodically patterned and quasiperiodically patterned pillar-arrayed surfaces have been calculated. Configurational entropy is zero for periodically patterned pillar-arrayed surfaces, whereas it is greater than zero for quasiperiodically patterned pillar-arrayed surfaces. The wetting morphology of liquid droplets on both periodically and quasiperiodically patterned pillar-arrayed surfaces has been summarized.

Finally, the influence of surface configurational entropy on the wetting morphology and dynamics of liquid droplets in experiments has been discussed. It is observed that the pillar-arrayed microstructured surfaces with configurational entropy greater than zero exhibit more complex wetting morphology of droplets compared to surfaces with zero configurational entropy. The configurational entropy proposed in this work may be helpful in understanding the mechanism of droplet wetting on microstructured surfaces and designing and characterizing microstructured surfaces.

Supplementary material. Supplementary material is available at https://doi.org/10.1017/flo.2024.10.

Declaration of interests. The authors declare no conflict of interest.

Funding statement. This work was jointly supported by the National Key R&D Program of China (grant nos 2022YFF0503500, 2022YFA1203200), the National Natural Science Foundation of China (grant nos. 12241205, 12032019, 12302349) and the Youth Innovation Promotion Association Chinese Academy of Sciences (grant no. 2020020).

Data availability statement. The data that support the findings of this study are available from the corresponding author upon reasonable request.

References

Alberti, G. & Desimone, A. 2005 Wetting of rough surfaces: a homogenization approach. *Proc. R. Soc.* A *Math. Phys. Engng Sci.* **461**, 79–97.

Apel-Paz, M. & Marmur, A. 1999 Spreading of liquids on rough surfaces. *Colloids Surf.* A *Physicochem. Engng Aspects* **146**, 273–279.

Beenker, F.P.M. 1982 *Algebraic Theory of Non-Periodic Tilings of the Plane by Two Simple Building Blocks: A Square and a Rhombus*. Eindhoven University of Technology.

Bercovici, M., Boyko, E., Gabay, I., Gat, A.D., Paratore, F. & Ramos, A. 2021 Shaping liquid films by dielectrophoresis. *Flow* **1**, E13.

Brockmann, P., Dörsam, E., Hussong, J., Roisman, I.V., Rothmann-Brumm, P. & Sauer, H.M. 2024 Gravure printing with a shear-rate-dependent ink. *Flow* **4**, E1.

Cazabat, A.M. & Stuart, M.A.C. 1986 Dynamics of wetting: effects of surface roughness. *J. Phys. Chem*. **90**, 5845–5849.

Cazabat, A.M. & Stuart, M.A.C. 1987 Dynamics of wetting on smooth and rough surfaces. *Prog. Colloid Polym. Sci*. **74**, 69–75.

Chamakos, N.T., Kavousanakis, M.E., Boudouvis, A.G. & Papathanasiou, A.G. 2016 Droplet spreading on rough surfaces: tackling the contact line boundary condition. *Phys. Fluids* **28**, 022105.

Chen, H., Ran, T., Gan, Y., Zhou, J., Zhang, Y., Zhang, L., Zhang, D. & Jiang, L. 2018*a* Ultrafast water harvesting and transport in hierarchical microchannels. *Nat. Mater*. **17**, 935–942.

Chen, E., Yuan, Q., Huang, X. & Zhao, Y.-P. 2016 Dynamic polygonal spreading of a droplet on a lyophilic pillar-arrayed surface. *J. Adhes. Sci. Technol*. **30**, 2265–2276.

Chen, E.H., Yuan, Q.Z. & Zhao, Y.-P. 2018*b* Topography-induced symmetry transition of droplets on quasi-periodically patterned surfaces. *Soft Matt*. **14**, 6198–6205.

Chu, K.-H., Xiao, R. & Wang, E.N. 2010 Uni-directional liquid spreading on asymmetric nanostructured surfaces. *Nat. Mater*. **9**, 413–417.

Courbin, L., Bird, J.C., Reyssat, M. & Stone, H.A. 2009 Dynamics of wetting: from inertial spreading to viscous imbibition. *J. Phys.: Condens. Matter* **21**, 464127.

Courbin, L., Denieul, E., Dressaire, E., Roper, M., Ajdari, A. & Stone, H.A. 2007 Imbibition by polygonal spreading on microdecorated surfaces. *Nat. Mater*. **6**, 661–664.

Dufour, R., Brunet, P., Harnois, M., Boukherroub, R., Thomy, V. & Senez, V. 2012 Zipping effect on omniphobic surfaces for controlled deposition of minute amounts of fluid or colloids. *Small* **8**, 1229–1236.

Duprat, C., Protiere, S., Beebe, A.Y. & Stone, H.A. 2012 Wetting of flexible fibre arrays. *Nature* **482**, 510–513.

Extrand, C.W., Moon, S.I., Hall, P. & Schmidt, D. 2007 Superwetting of structured surfaces. *Langmuir* **23**, 8882–8890.

de Gennes, P.G. 1985 Wetting: statics and dynamics. *Rev. Mod. Phys*. **57**, 827–863.

Jain, R. & Pitchumani, R. 2017 Fractal model for wettability of rough surfaces. *Langmuir* **33**, 7181–7190.

Jokinen, V., Leinikka, M. & Franssila, S. 2009 Microstructured surfaces for directional wetting. *Adv. Mater*. **21**, 4835–4838.

Kim, S.J., Moon, M.-W., Lee, K.-R., Lee, D.-Y., Chang, Y.S. & Kim, H.-Y. 2011 Liquid spreading on superhydrophilic micropillar arrays. *J. Fluid Mech*. **680**, 477–487.

Kumar, A. & Raj, R. 2017 Droplets on microdecorated surfaces: evolution of the polygonal contact line. *Langmuir* **33**, 4854–4862.

Li, P., Huang, X. & Zhao, Y.-P. 2022 Active control of electro-visco-fingering in Hele-Shaw cells using Maxwell stress. *iScience* **25**, 105204.

Li, P., Huang, X. & Zhao, Y.-P. 2023*a* Electro-capillary peeling of thin films. *Nat. Commun*. **14**, 6150.

Li, L., Wang, X., Deng, W., Yin, J., Li, X. & Guo, W. 2023*b* Hydrovoltaic energy from water droplets: device configurations, mechanisms, and applications. *Droplet* **2**, e77.

Lv, C., Yang, C., Hao, P., He, F. & Zheng, Q. 2010 Sliding of water droplets on microstructured hydrophobic surfaces. *Langmuir* **26**, 8704–8708.

Mandelbrot, B. 1918 Dimension und äußeres maß. *Math. Ann*. **79**, 157–179.

Mchale, G., Newton, M.I. & Shirtcliffe, N.J. 2009 Dynamic wetting and spreading and the role of topography. *J. Phys.: Condens. Matter* **21**, 464122.

Packham, D.E. 2003 Surface energy, surface topography and adhesion. *Intl J. Adhes. Adhes*. **23**, 437–448.

Penrose, R. 1979 Pentaplexity a class of non-periodic tilings of the plane. *Math. Intell*. **2**, 32–37.

Quéré, D. 2008 Wetting and roughness. *Annu. Rev. Mater. Res*. **38**, 71–99.

Raj, R., Adera, S., Enright, R. & Wang, E.N. 2014 High-resolution liquid patterns via three-dimensional droplet shape control. *Nat. Commun*. **5**, 4975.

Raj, R., Enright, R., Zhu, Y., Adera, S. & Wang, E.N. 2012 Unified model for contact angle hysteresis on heterogeneous and superhydrophobic surfaces. *Langmuir* **28**, 15777–15788.

Singh, M., Haverinen, H.M., Dhagat, P. & Jabbour, G.E. 2010 Inkjet printing–process and its applications. *Adv. Mater*. **22**, 673–685.

Stampfli, P. 1986 A dodecagonal quasi-periodic lattice in two dimensions. *Helv. Phys. Acta* **59**, 1260–1263.

Wang, J., Chen, W., Sun, J., Liu, C., Yin, Q., Zhang, L., Xianyu, Y., Shi, X., Hu, G. & Jiang, X. 2014*a* A microfluidic tubing method and its application for controlled synthesis of polymeric nanoparticles. *Lab on a Chip* **14**, 1673–1677.

Wang, L.-Z., Huang, X., Yuan, Q., Chen, L. & Yu, Y.-S. 2021 Dilute sodium dodecyl sulfate droplets impact on micropillar-arrayed non-wetting surfaces. *Phys. Fluids* **33**, 107103.

Wang, H., Wang, W., Li, L., Zhu, J., Wang, W., Zhang, D., Xie, Z., Fuchs, H., Lei, Y. & Chi, L. 2014*b* Surface microfluidic patterning and transporting organic small molecules. *Small* **10**, 2549–2552.

Xiao, R., Enright, R. & Wang, E.N. 2010 Prediction and optimization of liquid propagation in micropillar arrays. *Langmuir* **26**, 15070–15075.

https://doi.org/10.1017/flo.2024.10 Published online by Cambridge University Press

Xiao, R. & Wang, E.N. 2011 Microscale liquid dynamics and the effect on macroscale propagation in pillar arrays. *Langmuir* **27**, 10360–10364.

Yang, M., Wang, S.-Q., Liu, Z., Chen, Y., Zaworotko, M.J., Cheng, P., Ma, J.-G. & Zhang, Z. 2021 Fabrication of moisture-responsive crystalline smart materials for water harvesting and electricity transduction. *J. Am. Chem. Soc*. **143**, 7732–7739.

Yu, C., Schimelman, J., Wang, P., Miller, K.L., Ma, X., You, S., Guan, J., Sun, B., Zhu, W. & Chen, S. 2020 Photopolymerizable biomaterials and light-based 3D printing strategies for biomedical applications. *Chem. Rev*. **120**, 10695–10743.

Yu, X., Zhang, Y., Hu, R. & Luo, X. 2021 Water droplet bouncing dynamics. *Nano Energy* **81**, 105647.

Yuan, Q.Z., Huang, X.F. & Zhao, Y.-P. 2014 Dynamic spreading on pillar-arrayed surfaces: viscous resistance versus molecular friction. *Phys. Fluids* **26**, 092104.

Yuan, Q.Z. & Zhao, Y.P. 2013 Multiscale dynamic wetting of a droplet on a lyophilic pillar-arrayed surface. *J. Fluid Mech*. **716**, 171–188.

Yuk, H., Lu, B., Lin, S., Qu, K., Xu, J., Luo, J. & Zhao, X. 2020 3D printing of conducting polymers. *Nat. Commun*. **11**, 1604.

Zhao, Y.P. 2012 *Physical Mechanics of Surfaces and Interfaces*. Science Press.

Zhao, Y.P. 2014 Moving contact line problem: advances and perspectives. *Theor. Appl. Mech. Lett*. **4**, 034002.

Zhao, Y.P. 2016 *Modern Continuum Mechanics*. Science Press.

Cite this article: Chen E, Huang X, Zhao Y-P (2024). The configurational entropy of pillar-arrayed microstructured surfaces with spreading droplets. *Flow*, *4*, E12. doi:10.1017/flo.2024.10